

NON-EQUILIBRIUM THERMAL ENTANGLEMENT DYNAMICS OF HEISENBERG SYSTEMS

Fardin Kheirandish*, S. Javad Akhtarshenas[†] and Hamidreza Mohammadi[‡]

Department of Physics, University of Isfahan, Hezar Jarib Ave., Isfahan, Iran

Abstract

The effects of initial conditions and system parameters on entanglement dynamics and asymptotic entanglement for a two-qubit anisotropic XY Heisenberg system in the presence of an inhomogeneous magnetic field and spin-orbit interaction are investigated. We suppose that each qubit interacts with a separate thermal reservoir which is held in its own temperature. The effects of the parameters of the system and environment like spin-orbit interaction and temperature difference of reservoirs are also discussed.

PACS numbers: 03.67.Hk, 03.65.Ud, 75.10.Jm

* fardin_kh@phys.ui.ac.ir

† akhtarshenas@phys.ui.ac.ir

‡ h.mohammadi@sci.ui.ac.ir

I. INTRODUCTION

Entanglement is a central theme in quantum information processing which is first noted by Schrödinger [1, 2]. It strongly affects our conceptual implication on physics, and force us to change significantly our perspective of Nature. Entanglement implies that the best knowledge of the whole of a composite system may not include complete knowledge of its parts. In mathematical sense a pure state of pair of quantum systems is called entangled if it is unfactorizable. A mixed state ρ of a bipartite system is said to be separable or classically correlated if it can be expressed as a convex combination of uncorrelated states ρ_A and ρ_B of each subsystems i.e. $\rho = \sum_i \omega_i \rho_A^i \otimes \rho_B^i$ such that $\omega_i \geq 0$ and $\sum_i \omega_i = 1$, otherwise ρ is entangled [3, 4]. Entanglement has no classical analog and then can be considered as a uniquely quantum mechanical (non-classical) resource that plays a key role in many of the most interesting applications of quantum computation and quantum information processing such as: quantum teleportation, entanglement teleportation, quantum cryptography, and etc. [3, 4]. Performance the above mentioned tasks needs to quantifying and optimizing the amounts of the entanglements in a suitable multipartite quantum system. Many measures of entanglement have been introduced and analyzed [3, 5, 6], but the one most relevant to this work is entanglement of formation, which is intended to quantify the resources need to create a given entangled state [5]. For the case of a two-qubit system Wootters [5] has shown that entanglement of formation can be obtained explicitly as: $E(\rho) = \Xi[C(\rho)] = h\left(\frac{1+\sqrt{1+C^2}}{2}\right)$, where $h(x) = -x \log_2 x - (1-x) \log_2 (1-x)$ is the binary entropy function and $C(\rho) = \max\{0, 2\lambda_{max} - \sum_{i=1}^4 \lambda_i\}$ is the concurrence of the state, where λ_i s are positive square roots of the eigenvalues of the non-Hermitian matrix $R = \rho \tilde{\rho}$, and $\tilde{\rho}$ is defined by $\tilde{\rho} := (\sigma^y \otimes \sigma^y) \rho^* (\sigma^y \otimes \sigma^y)$. The function Ξ is a monotonically increasing function and ranges from 0 to 1 as C goes from 0 to 1, so that one can take the concurrence as a measure of entanglement in its own right. In the case that the state of the system is pure i.e. $\rho = |\psi\rangle\langle\psi|$, $|\psi\rangle = a|00\rangle + b|01\rangle + c|10\rangle + d|11\rangle$, the above formula is simplified to $C(|\psi\rangle) = 2 |ad - bc|$.

Real Quantum systems are not isolated from their environment. Unavoidable interaction between system and its environment cause to leakage the coherence of the system to environment and hence quantum-to-classical transition (see [7] and references therein) . More precisely, this interaction will, in general, create some entanglement between the states of

quantum system and the huge states of environment and as a consequence, quantum coherence initially localized within the system will become a shared property of composite system-environment state and can no longer be observed at the level of the system, leading to decoherence. Decoherence destroys the quantumness of the system and hence will decrease the useful entanglement between the parts of the system. A given dynamics for a composite quantum system can exhibit several distinct properties for asymptotic entanglement behavior, like: asymptotic death of entanglement(ADE) i.e. entanglement vanishes exponentially in time, entanglement sudden death (ESD) i.e. entanglement vanishes faster than local coherence of the system, asymptotically steady state entanglement(ASE) i.e the entanglement of the system reaches a stationary value, asymptotically, entanglement sudden birth (ESB) i.e. an initially separable state acquire entanglement asymptotically and etc [8, 9].

Among the numerous concepts considered to implement quantum bits (qubits), approaches based on semiconductor quantum dots (QDs) offer the great advantage that ultimately a miniaturized version of a quantum computer is feasible. Indeed, Loss and DiViencenzo initially proposed a quantum computer protocol based on electron spins trapped in semiconductor QDs in 1998 [10, 11, 12]. Here qubit is represented by the spin of a single electron in a QD, which can be initialized, manipulated, and read out by extremely sensitive devices. Such systems are more scalable and have a longer coherence time than other systems such as quantum optical and NMR systems. In this paper quantum entanglement dynamics of an open two-qubit system is realized by considering two electrons confined in two coupled quantum dots (CQDs) interacting with two separate reservoirs. We refer to this two-qubit system as "nanosystem" in the rest of the paper. Because of weak lateral confinement electrons can tunnel from one dot to the other and spin-spin and spin-orbit interactions between the two qubits exist. Thus we can model this nanosystem by a two-qubit spin chain including spin-orbit interaction. The spin chain is the natural candidates for the realization of entanglement and Heisenberg model is the simplest method for studying and investigating the behavior of the spin chains. On the other hand, in what follows we model the environment by a thermal reservoir and assume that the inter dot separation is large enough such that each dot couples to a separate thermal reservoir (bosonic bath). Here the bathes are assumed to be in thermodynamical equilibrium at different temperature $\beta_i = \frac{1}{k_B T_i}$. In general, there are two different ways for connecting the quantum dots to the reservoirs: (i)

"*direct geometry*"; where a high temperature bath is in contact with a QD in the presence of a strong magnetic field i.e. $b\Delta T > 0$ and (ii) "*indirect geometry*"; where a high temperature bath is in contact with a QD in the presence of a weak magnetic field i.e. $b\Delta T < 0$. The results show that the non-equilibrium thermal entanglement dynamics depends on the geometry of the system.

Entanglement properties of Heisenberg systems at thermal equilibrium (thermal entanglement) are extensively studied after Nielsen [13], who first studied the entanglement of a two-qubit Heisenberg XXX chain (see [14] and references therein) . For non-equilibrium thermal entanglement in spin systems, Eisler et al. [15] calculated the von Neumann entropy of a block of spins in XX spin chain in the presence of the energy current and showed that the enhancement of the amount of entanglement due to an energy current is possible. After them, the non-equilibrium thermal entanglement for steady state of some systems has been studied in a number of works [17, 18, 19]. For example, Quiroga in Ref. [20] considered a simple spin chain system (XXX-Heisenberg) which is in contact with two different heat reservoirs and showed that for the steady state, a temperature gradient can increase or decrease entanglement depending on the internal coupling strength between spins. Dynamics of non-equilibrium thermal entanglement of the same system has been studied by Sinaysky et al.[21]. They have derived an analytical expression for the density matrix of the system at a finite time. They also have shown that the system converges to a steady state, asymptotically and the amount of entanglement of the steady state takes its maximum value for unequal bath temperatures and also the local energy levels can maintain the entanglement at higher temperatures. However, the non-equilibrium thermal entanglement dynamics of more involved spin systems (e.g XY and XYZ Heisenberg systems) has not been considered, yet. In this paper, we will investigate dynamics of non-equilibrium thermal entanglement of a two qubit anisotropic XY Heisenberg system (nanosystem) in the presence of the inhomogeneous magnetic field and the spin orbit interaction. The influence of the parameters of the nanosystem (i.e. magnetic field (B), inhomogeneity of magnetic field(b), partial anisotropy(χ), mean coupling (J) and the spin-orbit interaction parameter (D)) and environmental parameters (i.e. temperatures T_1 and T_2 or equally T_M and ΔT , and the couplings γ_1 and γ_2) on the entanglement of the nanosystem is investigated. We have shown that, there is a steady state entanglement for asymptotically large times. The size of this steady state (asymptotic) entanglement and the dynamical behavior of entanglement

depend on the parameters of the model and also on the geometry of the system. Increasing the temperature difference ΔT , and mean temperature T_M , decrease the amount of asymptotic entanglement. We have also shown that, the size of T_M^{cr} (temperature over which the entanglement vanishes) and the amount of entanglement can be improved by adjusting the value of the spin-orbit interaction parameter D . The maximum entanglement ($C = 1$) can be achieved for the case of large values of D and zero temperature reservoirs ($T_1 = T_2 = 0$). Furthermore, we find that the indirect geometry is more suitable for creating and maintaining the entanglement. The results obtained here are consistent with those obtained in [14, 20, 21].

The paper is organized as follows. In Sec. II we introduce the Hamiltonian of the whole system-reservoir under the rotating wave approximation and then write the Markovian master equation governed on the nanosystem by tracing out the reservoirs' degrees of freedom. Ultimately, given some initial states, the density matrix of the nanosystem at a later time is derived exactly. The effects of initial conditions and system parameters on the dynamics of entanglement and entanglement of asymptotic state of the nanosystem are presented in Sec. III. Finally in Sec. IV a discussion concludes the paper.

II. THE MODEL AND THE HAMILTONIAN

The total Hamiltonian of the nanosystem which is interacting with two heat reservoirs (bosonic bath) is described by

$$\hat{H} = \hat{H}_S + \hat{H}_{B1} + \hat{H}_{B2} + \hat{H}_{SB1} + \hat{H}_{SB2}, \quad (1)$$

where \hat{H}_S is the Hamiltonian of the nanosystem, \hat{H}_{Bj} is the Hamiltonian of the j th bath ($j=1,2$) and \hat{H}_{SBj} denotes the system-bath interaction Hamiltonian. Nanosystem consists of two spin electron confined in a two coupled quantum dots and is described by a two-qubit anisotropic Heisenberg XY-model in the presence of an inhomogeneous magnetic field and spin-orbit interaction [14] with the following Hamiltonian

$$\begin{aligned} \hat{H}_S = & \frac{1}{2}(J_x \sigma_1^x \sigma_2^x + J_y \sigma_1^y \sigma_2^y + \mathbf{B}_1 \cdot \boldsymbol{\sigma}_1 + \mathbf{B}_2 \cdot \boldsymbol{\sigma}_2 \\ & + \mathbf{D} \cdot (\boldsymbol{\sigma}_1 \times \boldsymbol{\sigma}_2) + \delta \boldsymbol{\sigma}_1 \cdot \bar{\boldsymbol{\Gamma}} \cdot \boldsymbol{\sigma}_2) \end{aligned} \quad (2)$$

where $\boldsymbol{\sigma}_j = (\sigma_j^x, \sigma_j^y, \sigma_j^z)$ is the vector of Pauli matrices, \mathbf{B}_j ($j = 1, 2$) is the magnetic field on site j , J_μ ($\mu = x, y$) are the real coupling coefficients (the chain is anti-ferromagnetic (AFM))

for $J_\mu > 0$ and ferromagnetic (FM) for $J_\mu < 0$) and \mathbf{D} is Dzyaloshinski-Moriya vector, which is of first order in spin-orbit coupling and is proportional to the coupling coefficients (J_μ) and $\bar{\mathbf{T}}$ is a symmetric tensor which is of second order in spin-orbit coupling [22, 23, 24, 25]. For simplicity we assume $\mathbf{B}_j = B_j \hat{\mathbf{z}}$ such that $B_1 = B + b$ and $B_2 = B - b$, where b indicates the amount of inhomogeneity of magnetic field. The vector \mathbf{D} and the parameter δ are dimensionless, in system like coupled GaAs quantum dots $|\mathbf{D}|$ is of order of a few percent, while the order of last term is 10^{-4} and is negligible. If we take $\mathbf{D} = JD \hat{\mathbf{z}}$ and ignore the second order spin-orbit coupling, then the above Hamiltonian can be written as:

$$\begin{aligned} \hat{H}_S = & J\chi(\sigma_1^+ \sigma_2^+ + \sigma_1^- \sigma_2^-) + J(1 + iD)\sigma_1^+ \sigma_2^- + J(1 - iD)\sigma_1^- \sigma_2^+ \\ & + \left(\frac{B+b}{2}\right)\sigma_1^z + \left(\frac{B-b}{2}\right)\sigma_2^z, \end{aligned} \quad (3)$$

where $J := \frac{J_x + J_y}{2}$, is the mean coupling coefficient in the XY-plane, $\chi := \frac{J_x - J_y}{J_x + J_y}$, specifies the amount of anisotropy in the XY-plane (partial anisotropy, $-1 \leq \chi \leq 1$) and $\sigma^\pm = \frac{1}{2}(\sigma^x \pm i\sigma^y)$ are lowering and raising operators. The spectrum of H_S is easily obtained as

$$|\varepsilon_{1,2}\rangle = |\Psi^\pm\rangle = N^\pm \left(\left(\frac{b \pm \xi}{J(1-iD)} \right) |01\rangle + |10\rangle \right), \quad \varepsilon_{1,2} = \pm \xi, \quad (4)$$

$$|\varepsilon_{3,4}\rangle = |\Sigma^\pm\rangle = M^\pm \left(\left(\frac{B \pm \eta}{J\chi} \right) |00\rangle + |11\rangle \right), \quad \varepsilon_{3,4} = \pm \eta.$$

Here the eigenstates are expressed in the standard basis $\{|00\rangle, |01\rangle, |10\rangle, |11\rangle\}$. In the above equations $N^\pm = (1 + \frac{(b \pm \xi)^2}{J^2 + (JD)^2})^{-1/2}$ and $M^\pm = (1 + (\frac{B \pm \eta}{J\chi})^2)^{-1/2}$ are the normalization constants. Here we define, $\xi := (b^2 + J^2 + (JD)^2)^{1/2}$ and $\eta := (B^2 + (J\chi)^2)^{1/2}$, for later convenience.

The Hamiltonian of the reservoirs for each spin $j = 1, 2$ are given by

$$\hat{H}_{Bj} = \sum_n \omega_n \hat{b}_{nj}^\dagger \hat{b}_{nj}. \quad (5)$$

The interaction between the nanosystem and the bosonic bathes in the rotating wave approximation is as following

$$\hat{H}_{SBj} = \sigma_j^+ \sum_n g_n^{(j)} \hat{b}_{n,j} + \sigma_j^- \sum_n g_n^{(j)*} \hat{b}_{n,j}^\dagger \equiv \sum_\mu \hat{V}_{j,\mu} \hat{f}_{j,\mu} \quad (6)$$

The system operator $\hat{V}_{j,\mu}$ are chosen to satisfy $[\hat{H}_S, \hat{V}_{j,\mu}] = \omega_{j,\mu} \hat{V}_{j,\mu}$, and the $\hat{f}_{j,\mu}$ s are the random operators of reservoirs and act on the bath degrees of freedom. Physically, the

index μ corresponds to transitions between the internal levels of the nanosystem induced by the bath. The dynamics of the whole nanosystem+reservoirs is described by a density operator ($\hat{\sigma}$) satisfying the Liouville equation $\dot{\hat{\sigma}} = -i[\hat{H}, \hat{\sigma}]$. If the coupling strengths of the nanosystem and the environment are weak, the evolution of the nanosystem does not influence the states of the reservoirs and one can write $\hat{\sigma}(t) = \hat{\rho}(t)\hat{\rho}_{B1}(0)\hat{\rho}_{B2}(0)$ (irreversibility hypothesis), where $\hat{\rho}(t)$ is the reduced density matrix describing the nanosystem and each bosonic bath is described by a canonical density matrix of the form $\hat{\rho}_{Bj} = e^{-\beta_j \hat{H}_{Bj}}/Z$, where $Z = \text{Tr}(e^{-\beta_j \hat{H}_{Bj}})$ is the partition function of the j th bath.

In the Born-Markov approximation the master equation describing the dynamics of the reduced density matrix of the nanosystem is [16, 26]

$$\frac{d\hat{\rho}}{dt} = -i[\hat{H}_S, \hat{\rho}] + \mathcal{L}_1(\hat{\rho}) + \mathcal{L}_2(\hat{\rho}) \quad (7)$$

where $\mathcal{L}_j(\hat{\rho})$ are *dissipators* given by [26]

$$\mathcal{L}_j(\hat{\rho}) \equiv \sum_{\mu, \nu} J_{\mu, \nu}^{(j)}(\omega_{j, \nu}) \{ [\hat{V}_{j, \mu}, [\hat{V}_{j, \nu}^\dagger, \hat{\rho}]] - (1 - e^{\beta_j \omega_{j, \nu}}) [\hat{V}_{j, \mu}, \hat{V}_{j, \nu}^\dagger \hat{\rho}] \}. \quad (8)$$

here $J_{\mu, \nu}^{(j)}(\omega_{j, \nu})$ is the spectral density of the j th reservoir,

$$J_{\mu, \nu}^{(j)}(\omega_{j, \nu}) = \int_0^\infty d\tau e^{i\omega_{j, \nu} \tau} G_{\alpha\beta}(\tau) \quad (9)$$

where $G_{\alpha\beta}(\tau)$ is the environment self-correlation function,

$$G_{\alpha\beta}(\tau) = \text{Tr}_{Bj} [\rho_{Bj} \bar{f}_{j, \nu}(\tau) \hat{f}_{j, \mu}] \quad (10)$$

and $\bar{f}_{j, \nu}(\tau) = e^{-iH_{Bj}\tau} \hat{f}_{j, \mu}^\dagger e^{iH_{Bj}\tau}$. Spectral densities encapsulate the physical properties of the environment and play an immensely important role in the theoretical and experimental studies of the decoherence. In this paper, we will consider the bosonic thermal bath as an infinite set of harmonic oscillators and apply a Weisskopf-Wigner-like expression for spectral density such as $J^{(j)}(\omega_\mu) = \gamma_j(\omega_\mu) n_j(\omega_\mu)$ where $n_j(\omega_\mu) = (e^{\beta_j \omega_\mu} - 1)^{-1}$ denotes the thermal mean value of the number of excitations in the j th reservoir at frequency ω_μ and temperature $T_j = \frac{1}{\beta_j}$ and $\gamma_j(\omega_\mu)$ is the coupling strength of nanosystem and the j th reservoir. For simplicity we take $\gamma_j(\omega_\mu) = \gamma_j$. Thus, the dissipators $\mathcal{L}_j(\hat{\rho})$ become

$$\begin{aligned}
\mathcal{L}_j(\hat{\rho}) = & \sum_{\mu=1}^4 J^{(j)}(-\omega_\mu)(2\hat{V}_{j,\mu}\hat{\rho}\hat{V}_{j,\mu}^\dagger - \{\hat{\rho}, \hat{V}_{j,\mu}^\dagger\hat{V}_{j,\mu}\}_+) \\
& + \sum_{\mu=1}^4 J^{(j)}(\omega_\mu)(2\hat{V}_{j,\mu}^\dagger\hat{\rho}\hat{V}_{j,\mu} - \{\hat{\rho}, \hat{V}_{j,\mu}\hat{V}_{j,\mu}^\dagger\}_+)
\end{aligned} \tag{11}$$

with the transition frequencies

$$\begin{aligned}
\omega_1 &= \xi - \eta, & \omega_4 &= -\omega_1, \\
\omega_2 &= \xi + \eta, & \omega_3 &= -\omega_2,
\end{aligned} \tag{12}$$

and the transition operators

$$\begin{aligned}
\hat{V}_{j,1} &= a_{j,1}|\Psi^+\rangle\langle\Sigma^+|, \\
\hat{V}_{j,2} &= a_{j,2}|\Psi^+\rangle\langle\Sigma^-|,
\end{aligned} \tag{13}$$

$$\begin{aligned}
\hat{V}_{j,3} &= a_{j,3}|\Psi^-\rangle\langle\Sigma^+|, \\
\hat{V}_{j,4} &= a_{j,4}|\Psi^-\rangle\langle\Sigma^-|,
\end{aligned} \tag{14}$$

where

$$\begin{aligned}
|a_{j,1}|^2 &= |a_{j,4}|^2 = \frac{1}{2\xi\eta}(\xi\eta + J^2\chi + (-1)^j Bb), \\
|a_{j,2}|^2 &= |a_{j,3}|^2 = \frac{1}{2\xi\eta}(\xi\eta - J^2\chi - (-1)^j Bb),
\end{aligned} \tag{15}$$

can be obtained from the spectrum of the nanosystem Hamiltonian.

The quantum master equation (7) has an important property, when the spectrum of \hat{H}_s (see eq.(4)) is non-degenerate: In the energy basis, $\{|\varepsilon_i\rangle\}_{i=1}^4$, the equations for diagonal elements decouple from nondiagonal ones [16]. Furthermore, nondiagonal elements are not coupled and the time dependence of these elements has the simple form

$$\rho_{i,j}(t) = \rho_{i,j}(0)e^{\alpha_{ij}t}, \tag{16}$$

where $\alpha_{i,j} \in \mathbb{C}$ are determined by the nanosystem parameters. The equations for diagonal elements have the following form

$$\dot{R}(t) = BR(t), \tag{17}$$

where dot denotes the time derivative, $R(t) = (\rho_{11}(t), \rho_{22}(t), \rho_{33}(t), \rho_{44}(t))^T$ and B is the time independent 4×4 matrix

$$B = \begin{pmatrix} -(X_1^- + Y_2^-) & 0 & X_1^+ & Y_2^+ \\ 0 & -(X_1^+ + Y_2^+) & Y_2^- & X_1^- \\ X_1^- & Y_2^+ & -(X_1^+ + Y_2^-) & 0 \\ Y_2^- & X_1^+ & 0 & -(X_1^- + Y_2^+) \end{pmatrix}, \quad (18)$$

where

$$\begin{aligned} X_\mu^\pm &= 2 \sum_{j=1,2} J^{(j)}(\mp \omega_\mu) |a_{j,1}|^2, \\ Y_\mu^\pm &= 2 \sum_{j=1,2} J^{(j)}(\mp \omega_\mu) |a_{j,2}|^2. \end{aligned} \quad (19)$$

The analytical solution of the equation (17) in the energy basis is given by

$$R(t) = M(t)R(0) \quad (20)$$

where $M(t) = [m_{ij}]_{4 \times 4}$, and the elements m_{ij} are defined by

$$\begin{aligned}
m_{11} &= \frac{1}{X_1 Y_2} (X_1^+ + X_1^- e^{-tX_1}) (Y_2^+ + Y_2^- e^{-tY_2}), \\
m_{12} &= \frac{1}{X_1 Y_2} (1 - e^{-tX_1}) (1 - e^{-tY_2}) X_1^+ Y_2^+, \\
m_{13} &= \frac{1}{X_1 Y_2} (1 - e^{-tX_1}) X_1^+ (Y_2^+ + Y_2^- e^{-tY_2}), \\
m_{14} &= \frac{1}{X_1 Y_2} (X_1^+ + X_1^- e^{-tX_1}) (1 - e^{-tY_2}) Y_2^-, \\
m_{21} &= \frac{1}{X_1 Y_2} (1 - e^{-tX_1}) (1 - e^{-tY_2}) X_1^- Y_2^-, \\
m_{22} &= \frac{1}{X_1 Y_2} (X_1^- + X_1^+ e^{-tX_1}) (Y_2^- + Y_2^+ e^{-tY_2}), \\
m_{23} &= \frac{1}{X_1 Y_2} (X_1^- + X_1^+ e^{-tX_1}) (1 - e^{-tY_2}) Y_2^-, \\
m_{24} &= \frac{1}{X_1 Y_2} (1 - e^{-tX_1}) X_1^- (Y_2^- + Y_2^+ e^{-tY_2}), \\
m_{31} &= \frac{1}{X_1 Y_2} (1 - e^{-tX_1}) X_1^- (Y_2^+ + Y_2^- e^{-tY_2}), \\
m_{32} &= \frac{1}{X_1 Y_2} (X_1^- + X_1^+ e^{-tX_1}) (1 - e^{-tY_2}) Y_2^+, \\
m_{33} &= \frac{1}{X_1 Y_2} (X_1^- + X_1^+ e^{-tX_1}) (Y_2^+ + Y_2^- e^{-tY_2}), \\
m_{34} &= \frac{1}{X_1 Y_2} (1 - e^{-tX_1}) (1 - e^{-tY_2}) X_1^- Y_2^+, \\
m_{41} &= \frac{1}{X_1 Y_2} (X_1^+ + X_1^- e^{-tX_1}) (1 - e^{-tY_2}) Y_2^-, \\
m_{42} &= \frac{1}{X_1 Y_2} (1 - e^{-tX_1}) X_1^+ (Y_2^- + Y_2^+ e^{-tY_2}), \\
m_{43} &= \frac{1}{X_1 Y_2} (1 - e^{-tX_1}) (1 - e^{-tY_2}) X_1^+ Y_2^-, \\
m_{44} &= \frac{1}{X_1 Y_2} (X_1^+ + X_1^- e^{-tX_1}) (Y_2^- + Y_2^+ e^{-tY_2}),
\end{aligned} \tag{21}$$

here we have defined: $X_\mu = X_\mu^+ + X_\mu^-$ and $Y_\mu = Y_\mu^+ + Y_\mu^-$.

There is a singular point $\xi = \eta$, for which the spectrum (4) becomes degenerate and the above solution is not valid. The state of the system is not well defined at this critical point. This critical point assigns a critical value for the parameters of the nanosystem such as critical magnetic field (B_c), critical parameter of inhomogeneity of magnetic field (b_c), critical spin-orbit interaction parameter (D_c) and etc. The behavior of the entanglement of the system changes abruptly when the parameters cross their critical values (see section

III).

In the following we will examine a class of bipartite density matrices having the following standard form as the initial state of the system [27]

$$\hat{\rho}_s(0) = \begin{pmatrix} \mu_+ & 0 & 0 & \nu \\ 0 & w_1 & z & 0 \\ 0 & z^* & w_2 & 0 \\ \nu & 0 & 0 & \mu_- \end{pmatrix}. \quad (22)$$

These kind of density matrix are called X states class and arises naturally in a wide variety of physical situations. This class contains some important subsets like the pure Bell states, the states which can be expressed as a mixture of Bell states, Werner states and so on. If the initial state, $\hat{\rho}_s(0)$, belongs to the set of X states (22) then Eq (4) guarantees that $\hat{\rho}_s(t)$ given by Eqs. (23 and 16) also belongs to the same set. Therefore, the only non-vanishing off diagonal components of the density matrix in the energy basis are

$$\begin{aligned} \rho_{12}(t) &= \rho_{12}(0)e^{-2i\xi t - t(X_1+Y_2)/2}, & \rho_{21}(t) &= \rho_{12}(t)^*, \\ \rho_{34}(t) &= \rho_{34}(0)e^{-2i\eta t - t(X_1+Y_2)/2}, & \rho_{43}(t) &= \rho_{34}(t)^*. \end{aligned} \quad (23)$$

Knowing the density matrix we can calculate the concurrence $C(\rho(t)) = \max\{0, 2\lambda_{max}(t) - \sum_{i=1}^4 \lambda_i(t)\}$ where,

$$\begin{aligned} \lambda_{1,2}(t) &= |\sqrt{\rho_{s11}(t)\rho_{s44}(t)} \pm |\rho_{s14}(t)| |, \\ \lambda_{3,4}(t) &= |\sqrt{\rho_{s22}(t)\rho_{s33}(t)} \pm |\rho_{s23}(t)| |. \end{aligned} \quad (24)$$

Unfortunately, the $\lambda_i(t)$ s depend on the parameters involved. This prevents us from writing an analytical expression for concurrence. But it is possible to evaluate concurrence, numerically for a given set of the parameters. The results are shown in Figs. 1-7. Figs. 1-3 depict the dynamical behavior of concurrence versus parameters of the nanosystem and reservoirs and Figs. 4-7 illustrate the asymptotical behavior of the concurrence versus parameters of the nanosystem and reservoirs. Without loss of generality we can assume that $J > 0$, since the above formula are invariant under substitution $J \rightarrow -J$. This means that the dynamical behavior of the FM chain is the same as the AFM chain.

A. Asymptotic case

For a class of states, $\hat{\rho}_{st}$, the dissipative and decoherence mechanisms (second and third terms in the master equation (7)) compensate the unitary dynamics which is governed by nanosystem Hamiltonian (first term in master equation (7)) i.e. $i[\hat{H}_S, \hat{\rho}_{st}] = \mathcal{L}_1(\hat{\rho}_{st}) + \mathcal{L}_2(\hat{\rho}_{st})$ or $\frac{d}{dt}\hat{\rho}_{st} = 0$. These states are called stationary states because they are constant in time. If there exist such a stationary state solution for the master equation, the system tends to it asymptotically in large time limit i.e. $\lim_{t \rightarrow \infty} \hat{\rho}(t) \rightarrow \hat{\rho}_{asym.} = \hat{\rho}_{st}$. For the present system (thermal reservoirs and interacting nanosystem), nondiagonal elements (16) vanish asymptotically at large time limit and hence $\hat{\rho}(t)$ converges to a diagonal density matrix (in the energy basis) with elements not depending on the initial conditions:

$$\hat{\rho}_{asym.} = \frac{1}{X_1 Y_2} \text{diagonal}(X_1^+ Y_2^+, X_1^- Y_2^-, X_1^- Y_2^+, X_1^+ Y_2^-). \quad (25)$$

The asymptotic concurrence is given by $C(\rho_{asym.}) = C^\infty = \max\{0, 2\lambda_{max} - \sum_{i=1}^4 \lambda_i\}$ with

$$\begin{aligned} \lambda_{1,2} &= |\sqrt{\rho_{s11}^{asym.} \rho_{s44}^{asym.}} \pm |\rho_{s14}^{asym.}| |, \\ \lambda_{3,4} &= |\sqrt{\rho_{s22}^{asym.} \rho_{s33}^{asym.}} \pm |\rho_{s23}^{asym.}| |, \end{aligned} \quad (26)$$

where

$$\begin{aligned} \rho_{s11}^{asym.} &= \frac{1}{2\eta X_1 Y_2} ((\eta + B)X_1^- Y_2^+ + (\eta - B)X_1^+ Y_2^-), \\ \rho_{s14}^{asym.} &= \frac{J\chi}{2\eta X_1 Y_2} (X_1^- Y_2^+ - X_1^+ Y_2^-) = \rho_{s41}^{asym.}, \\ \rho_{s22}^{asym.} &= \frac{1}{2\xi X_1 Y_2} ((\xi + b)X_1^+ Y_2^+ + (\xi - b)X_1^- Y_2^-), \\ \rho_{s23}^{asym.} &= \frac{J(1 + iD)}{2\xi X_1 Y_2} (X_1^+ Y_2^+ - X_1^- Y_2^-) = (\rho_{s32}^{asym.})^*, \\ \rho_{s33}^{asym.} &= \frac{1}{2\xi X_1 Y_2} ((\xi - b)X_1^+ Y_2^+ + (\xi + b)X_1^- Y_2^-), \\ \rho_{s44}^{asym.} &= \frac{1}{2\eta X_1 Y_2} ((\eta - B)X_1^- Y_2^+ + (\eta + B)X_1^+ Y_2^-). \end{aligned} \quad (27)$$

There is an interesting limiting case for which the coupled QDs are in contact with two independent reservoirs at identical temperatures ($\beta_1 = \beta_2 = \beta$). In this case, it is easy to show that

$$\begin{aligned}\frac{X_1^+}{X_1} &= \frac{e^{\beta\omega_1}}{e^{\beta\omega_1} + 1}, & \frac{X_1^-}{X_1} &= \frac{1}{e^{\beta\omega_1} + 1} \\ \frac{Y_2^+}{Y_2} &= \frac{e^{\beta\omega_2}}{e^{\beta\omega_2} + 1}, & \frac{Y_2^-}{Y_2} &= \frac{1}{e^{\beta\omega_2} + 1}.\end{aligned}$$

By substituting these relations into the Eq. (25), the reduced density matrix $\hat{\rho}_{asym.}$ takes the thermodynamical canonical form for a system described by the Hamiltonian \hat{H}_S at temperature $T = \beta^{-1}$, as expected. This means that

$$\hat{\rho}_{asym.}(\Delta T = 0) \equiv \hat{\rho}_T = \frac{e^{-\beta H_S}}{Z}, \quad (28)$$

where $Z = Tr(e^{-\beta H_S})$ is the partition function. Thermal entanglement properties of such systems have been studied substantially, in our previous work [14]. Thus, for the special case $\Delta T = 0$, the results coincide with the results of Ref.[14].

III. RESULTS

The non-equilibrium thermal concurrence as a function of time for three values of temperature difference ($\Delta T = T_1 - T_2$) and for a fixed value of mean temperature ($T_M = \frac{T_1 + T_2}{2}$) are plotted in Fig. 1, for the case of "direct geometry" of connection ($b\Delta T > 0$). The presence of temperature difference has not effective influence on the dynamics of entanglement at early times of evolution, but changes effectively the behavior of the asymptotic entanglement (which is more evident from Figs. 4-7). Fig. 2 depicts the variation of entanglement dynamics for some values of T_M and for a fixed ΔT in the case of "direct geometry" of connection ($b\Delta T > 0$). By Increasing T_M , thermal fluctuations suppress quantum fluctuations and hence decrease coherent oscillations at early times of evolution and also decrease asymptotic entanglement.

Perhaps surprisingly, the decoherence due to environmental interaction does not prevent the creation of a steady state level of entanglement, regardless of the initial state of the system. This is demonstrated in figure 3 which shows the time evolution of the non-equilibrium thermal concurrence for a given set of parameters and for four different initial states: (i) a maximally entangled state, the Bell state, $|\psi(0)\rangle = \frac{1}{\sqrt{2}}(|01\rangle + |10\rangle)$ (ii) a separable state, $|\psi(0)\rangle = |01\rangle$ (iii) a mixed state, defined as an equal mixture of a Bell state and a product state, e.g. $\rho_s(0) = \frac{1}{4}(|00\rangle + |11\rangle)(\langle 00| + \langle 11|) + \frac{1}{2}|01\rangle\langle 01|$ and finally (iv) an unpolarized

state, $\rho_s(0) = \frac{1}{4}I$. Despite the presence of decoherence (due to interaction with environment) the results of figure 3 show that the concurrence reaches the same steady state value, C^∞ (after some oscillatory behavior) for a given set of parameters, regardless of initial state of the system. Clearly the Heisenberg interaction in the Eq. (3) serves to maintain an entangled asymptotic state despite the presence of decoherence. At early times of evolution the amount of D determines the frequency of oscillations. Each plot in Fig. 3 contains two cases a) $D < D_c$, in this case asymptotic value of entanglement decreases with D and b) $D > D_c$, in this case asymptotic value of entanglement increases as D increases.

In Fig. 4, the asymptotic non-equilibrium thermal concurrence is plotted versus T_M and D for different values of ΔT . For the case of identical temperatures ($\Delta T = 0$) the results are the same as ref. [14], as mentioned in the previous section. This figure shows that there is a critical mean temperature ($T_M^{cr.}$) over which entanglement vanishes (ESD phenomenon). The size of $T_M^{cr.}$ and the amount of entanglement can be improved by increasing D . For Small values of D ($D < D_c$), an increase in ΔT increases the size of $T_M^{cr.}$ i.e entanglement can exists in higher mean temperatures due to existence of temperature difference of reservoirs (environment induced entanglement).

The variation of the asymptotic non-equilibrium thermal concurrence as a function of ΔT and D for fixed values of T_M and b is illustrated in Fig. 5. The behavior of concurrence is dependent on the geometry of connection. For the case of "direct geometry" ($b\Delta T > 0$) and for $D < D_c$, no entanglement is observed but for the same geometry and for $D > D_c$ the amount of entanglement is nonzero and it increases as D or ΔT increases. For the case of "indirect geometry" ($b\Delta T < 0$), there is a nonzero entanglement for all values of D . The amount of entanglement is an increasing function of D and increases with ΔT for the values of $\Delta T \leq \frac{T_M}{2}$ and decreases with ΔT for the values of $\frac{T_M}{2} < \Delta T \leq T_M$.

Figs. 6 and 7 show the behavior of the asymptotic non-equilibrium thermal concurrence versus T_M and ΔT for different values of D and for the symmetric ($b = 0$) and nonsymmetric ($b \neq 0$) cases, respectively. Both figures reveal that, increasing D cause to the appearance of entanglement in the larger region of $T_M - \Delta T$ plane. The departure between symmetric (Fig. 6) and nonsymmetric (Fig. 7) case is more obvious for $D < D_c$. For nonsymmetric case, Fig.7 shows that the "indirect geometry" of connection is more suitable for creating entanglement when $D < D_c$. In both symmetric and nonsymmetric cases, maximum entanglement ($C = 1$) can be achieved in the case of identical temperatures ($\Delta T = 0$), zero mean

temperature ($T_M = 0$) (i.e when both of reservoirs are in the ground state ($T_1 = T_2 = 0$)) and large values of D (it is in agreement with the results of [14]).

IV. DISCUSSION

The Dynamics of non-equilibrium thermal entanglement of an open two-qubit nanosystem is investigated. The inter-qubit interaction is considered as the Heisenberg interaction in the presence of inhomogeneous magnetic field and spin-orbit interaction (arises from the Dzyaloshinski- Moriya (DM) anisotropic antisymmetric interaction). Each qubit interacts with separate thermal reservoir (bosonic bath) which is held in its own temperature. The effects of the parameters of the model, including the parameters of the nanosystem (especially, the parameter of the spin orbit interaction (D)) and environmental parameters (particularly, mean temperature T_M and temperature difference ΔT), on the non-equilibrium thermal entanglement dynamics of the nanosystem is investigated, by solving the quantum Markov-Born master equation of the nanosystem. An analytical solution of the master equation is derived and then entanglement dynamics and asymptotic entanglement of the nanosystem versus the parameters of the model is studied. Resolving the entanglement dynamics allowed us to distinguish between entanglement induced by the interaction and by the environment. The results show that, decoherence induced by thermal bathes are competing with inter-qubit interaction terms to create a steady state level of entanglement, as measured by the concurrence. The size of this steady state (asymptotic) entanglement and the dynamical behavior of entanglement are dependent on the parameters of the model and also depend on the geometry of connection. Increasing temperature difference ΔT , and mean temperature T_M , kill the asymptotic entanglement. Indeed, thermal fluctuations suppress the quantum fluctuations (i.e. all quantum effects such as the entanglement and local coherence), and hence the entanglement of the system dies at a critical temperature $T_M^{cr.}$ (ESD). We have shown that, the size of $T_M^{cr.}$ and the amount of entanglement can be enhanced by choosing a suitable value of spin-orbit interaction parameter D . The maximum entanglement ($C = 1$) can be achieved for the case of large values of D and zero temperature reservoirs ($T_1 = T_2 = 0$). For physical realization of the model we address a two coupled quantum dots which are interacting with two independent thermal bathes. Furthermore, we find that the indirect geometry of connection is more suitable for creating and maintaining

the entanglement. In this case, the heat current between two QDs is substantially decreased but the concurrence can enhance by temperature difference ΔT [20]. For the special case $\Delta T = 0$, our results confirm the results of [14]. The results of [20, 21] are also obtained for the special case of $D = \chi = 0$ and by considering $b = \epsilon_1 - \epsilon_2$. The results can provide useful recipes for realistic quantum information processing in noisy and non-equilibrium environments.

-
- [1] A. Einstein, B. Podolsky and N. Rosen, Phys. Rev. **47**, 777 (1935)
 - [2] E. Schrödinger, Naturwiss. **23**, 807 (1935)
 - [3] M. A. Nielsen and I. L. Chuang, *Quantum computation and quantum information* (Cambridge University Press, U.K., 2004)
 - [4] J. Audretsch, *Entangled systems*, (WILEY-VCH Verlag, Weinheim, 2007)
 - [5] S. Hill and W. K. Wootters, Phys. Rev. Lett. **78** (1997); W. K. Wootters, Phys. Rev. Letts., **80**, 2245 (1998)
 - [6] J. Eisert, Ph.D thesis, The University of Postdam, 2001 (unpublished)
 - [7] M. Schlosshauer, *Decoherence and the quantum to classical transition*, (Springer, 2007)
 - [8] R.C. Drumond and M. O. Terra Cunha, e-print quant-ph/0809.4445
 - [9] M. O. Terra Cunha, New J. Phys. **9**, 237 (2007)
 - [10] D. Loss and D.P. Divincenzo, Phys. Rev. A **57**, 120 (1998)
 - [11] D. DiVincenzo, Phys. Rev. A **51**, 1015 (1995)
 - [12] W. A. Coish and D. Loss, e-print cond-mat/0606550 (1998) and G. Burkard, D. Loss and D. P. Divincenzo , Phys. Rev. B **59**, 2070 (2002)
 - [13] M. A. Nielsen, e-print quant-ph/0011036
 - [14] F. Kheirandish, S. J. Akhtarshenas and H. Mohammadi, Phys. Rev. A **77**, 042309 (2008)
 - [15] V. Eisler and Z. Zimboras, Phys. Rev. A **71**, 042318 (2005)
 - [16] H. P. Breuer and F. Petruccione, *The Theory of Open Quantum Systems*, (Oxford University Press, Oxford, 2002)
 - [17] J. Wang, H. Batelaan, J. Ponday and A. F. Starace, J. Phys. B: At. Mol. Opt Phys. **39**, 4343 (2006)
 - [18] M. Scala, R. Migliore and A. Messina, e-print quant-ph/0806.4852
 - [19] T. Proson, New J. Phys. **10**, 0423026
 - [20] L. Quiroga and F. J. Rodríguez, Phys. Rev. A **75**, 032308 (2007)
 - [21] I. Sinaysky, F. Petruccione and D. Bargarth, Phys. Rev. A **78**, 062301 (2008)
 - [22] I. Dzyaloshinski, J. Phys. Chem. Solids **4**, 241 (1958)
 - [23] T. Moriya, Phys. Rev. **117**, 635 (1960)
 - [24] T. Moriya, Phys. Rev. Lett. **4**, 228 (1960)

- [25] T. Moriya, Phys. Rev. **120**, 91 (1960)
- [26] M. Goldman, J. Magn. Reson. **149**, 160 (2001)
- [27] The subscript "s" denotes the standard computational basis $\{|00\rangle, |01\rangle, |10\rangle, |11\rangle\}$.

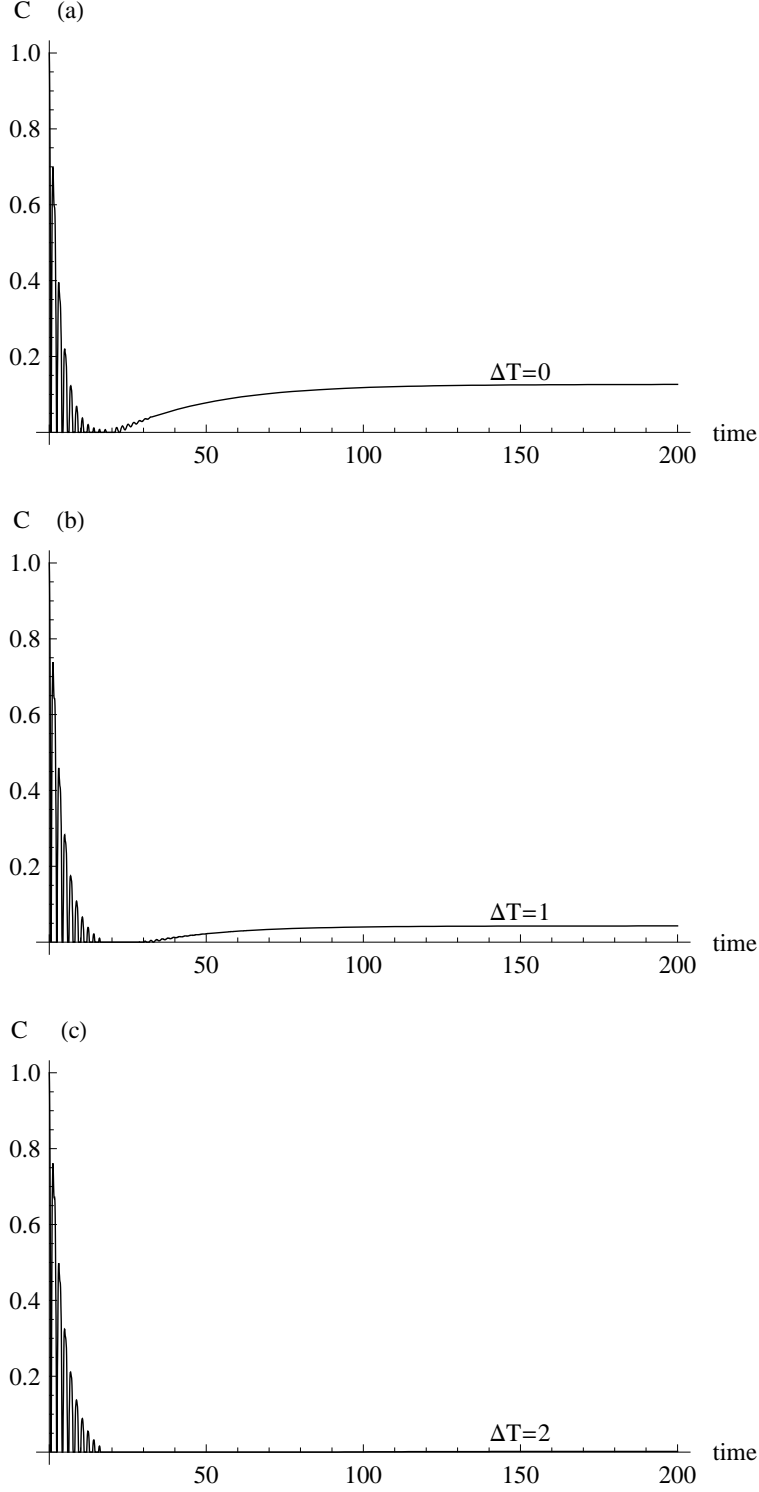


FIG. 1: Dynamics of non-equilibrium concurrence for the initial reduced density matrix $\rho_s(0) = \frac{1}{\sqrt{2}}(|01\rangle\langle 01| + |10\rangle\langle 10|)$. The parameters of the model are chosen to be $\gamma_1 = \gamma_2 = 0.02$, $J = 1$, $\chi = 0.9$, $B = 2$, $b = 1$, $T_M = 1.5$ and for different values of temperature difference ΔT : (a) $\Delta T = 0$ (b) $\Delta T = 1$ (c) $\Delta T = 2$. All parameters are dimensionless.

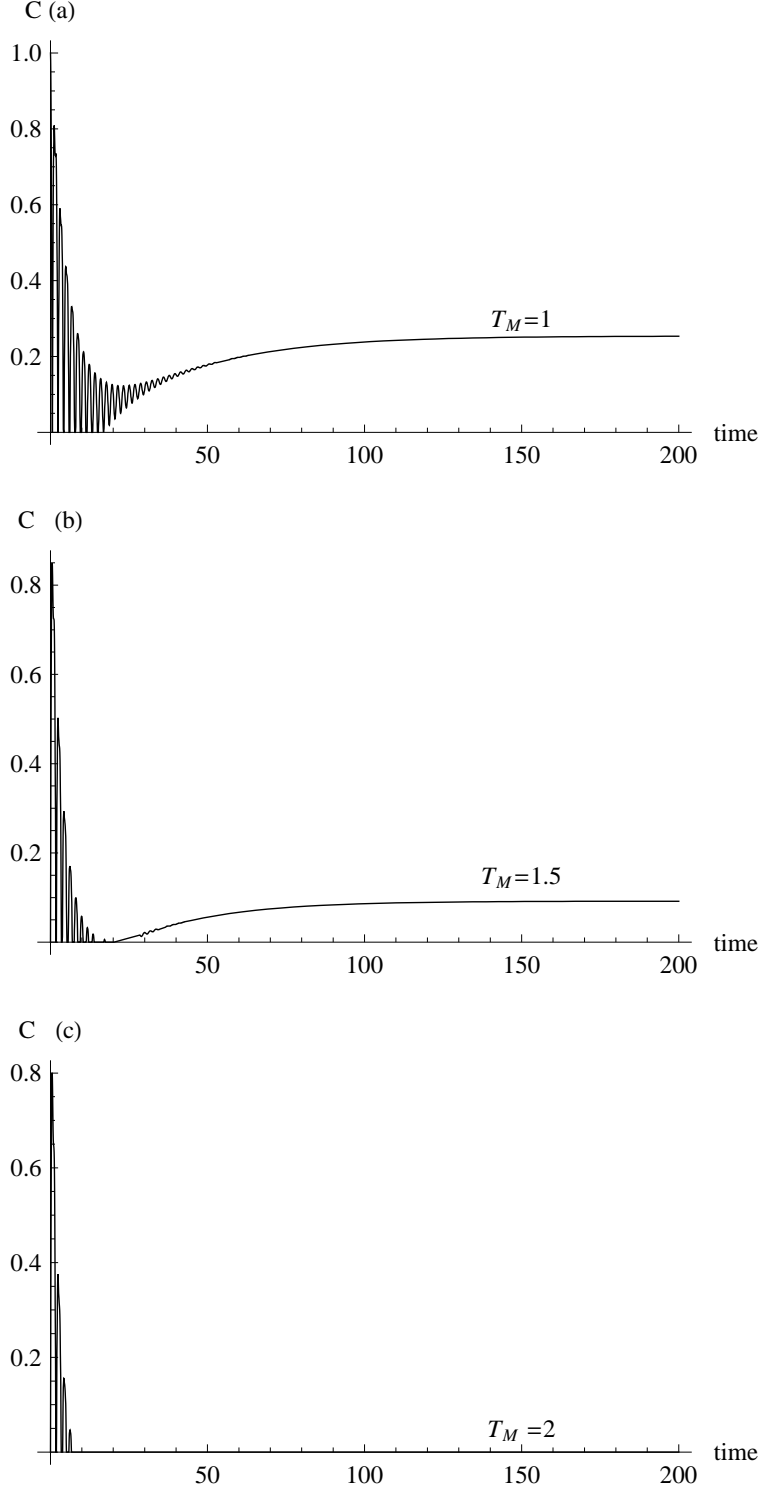


FIG. 2: Dynamics of non-equilibrium concurrence for the initial reduced density matrix $\rho_s(0) = \frac{1}{\sqrt{2}}(|01\rangle\langle 01| + |10\rangle\langle 10|)$. The parameters of the model are chosen to be $\gamma_1 = \gamma_2 = 0.02$, $J = 1$, $\chi = 0.9$, $B = 2$, $b = 1$, $\Delta T = 0.5$ and for different values of mean temperature T_M : (a) $T_M = 1$ (b) $T_M = 1.5$ (c) $T_M = 2$. All parameters are dimensionless.

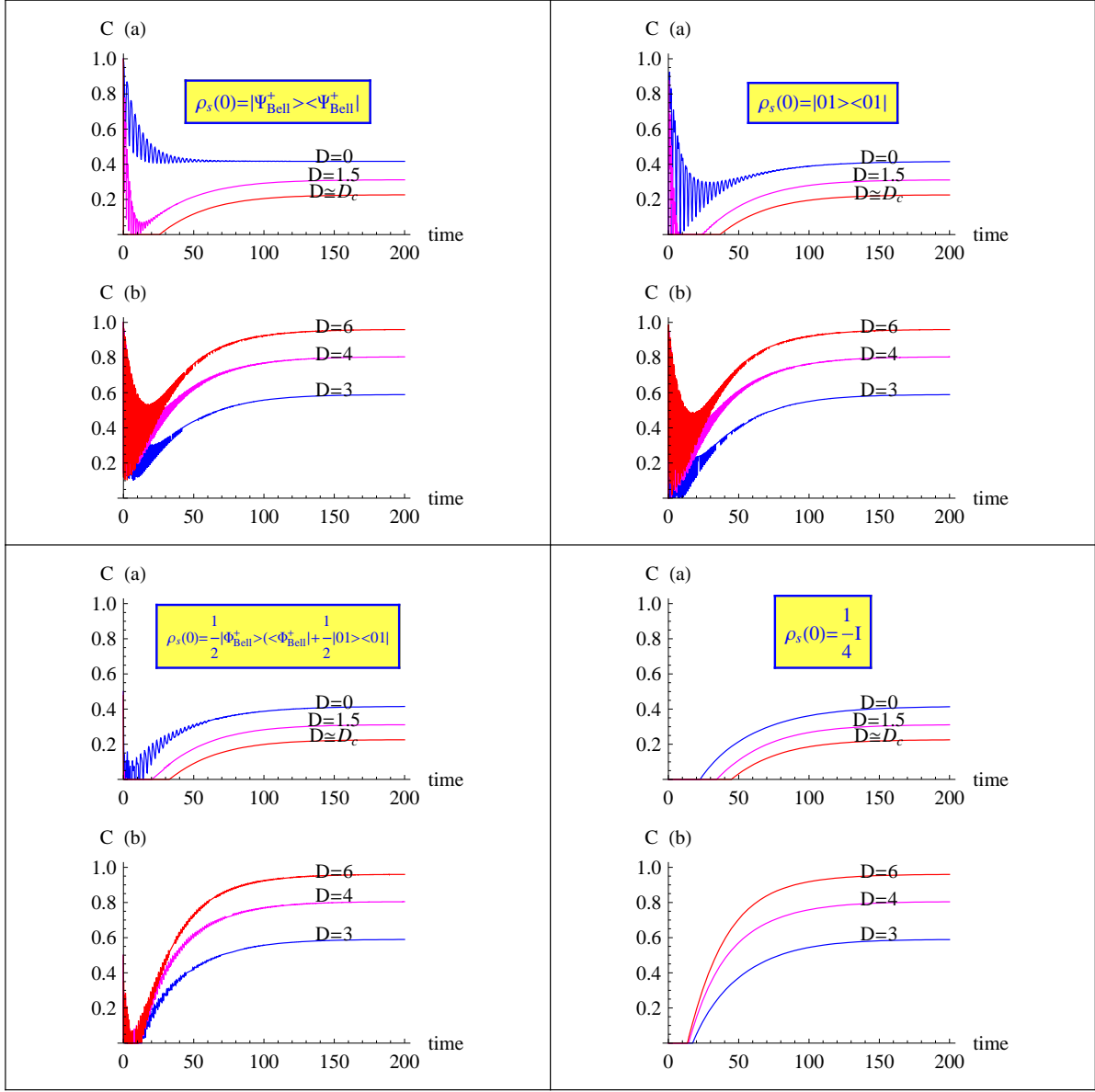


FIG. 3: (Color online) Dynamics of non-equilibrium concurrence for different values of D and different initial state. The parameters of the model are chosen to be $\gamma_1 = \gamma_2 = 0.02$, $J = 1$, $\chi = 0.9$, $B = 2$, $b = 0.5$, $T_M = 1$ and $\Delta T = 0.5$. Each plot contains two graphs for (a) $D < D_c$ (b) $D > D_c$ ($D_c \simeq 1.8868$). All parameters are dimensionless.

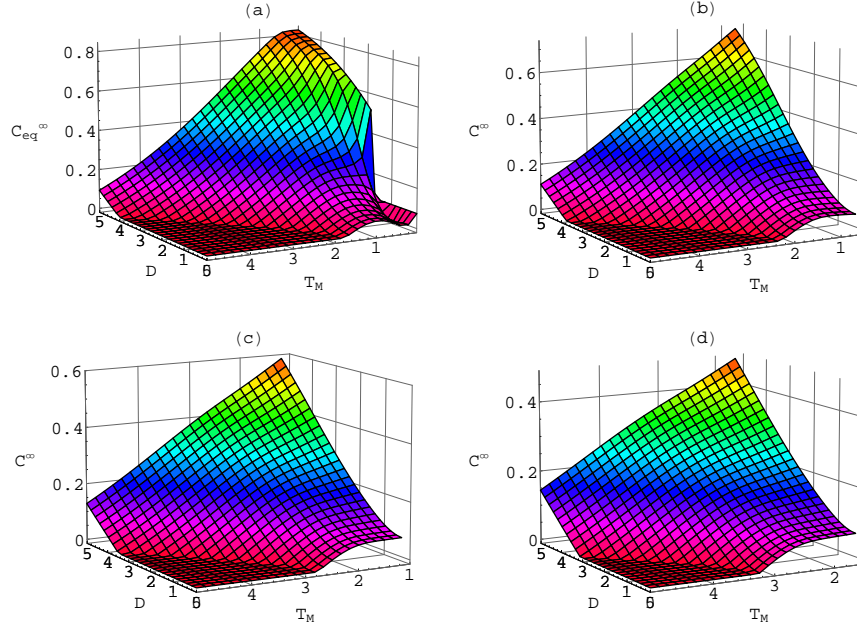


FIG. 4: (Color online) Asymptotic entanglement vs. T_M and D , The parameters of the model are chosen to be $\gamma_1 = \gamma_2 = 0.02$, $B = 4$, $J = 1$, $\chi = 0.3$ and $b = -3.5$ for (a) $\Delta T = 0$ (b) $\Delta T = 1$ (c) $\Delta T = 2$ (d) $\Delta T = 3$ ($D_c \simeq 1.68523$). All parameters are dimensionless.

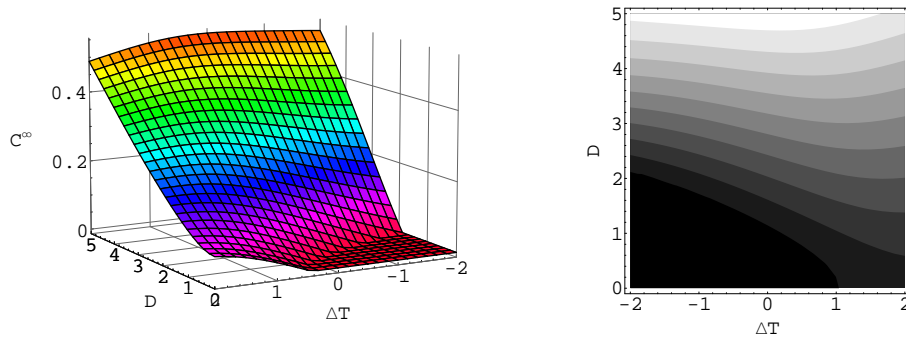


FIG. 5: (Color online) Asymptotic entanglement vs. ΔT and D . The parameters of the model are chosen to be $\gamma_1 = \gamma_2 = 0.02$, $B = 4$, $J = 1$, $\chi = 0.3$ and $b = -3.5$ and $T_M = 2$ ($D_c \simeq 1.68523$). All parameters are dimensionless.

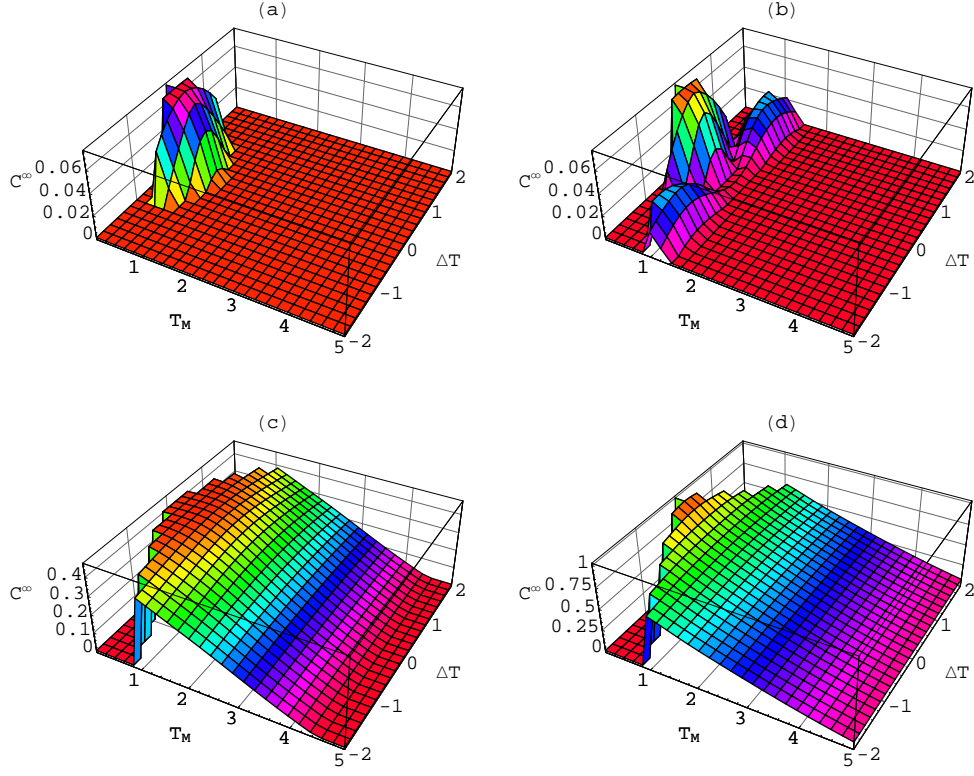


FIG. 6: (Color online) Asymptotic entanglement vs. T_M and ΔT . The parameters of the model are chosen to be $\gamma_1 = \gamma_2 = 0.02$, $B = 4$, $J = 1$, $\chi = 0.3$ and $b = 0$ for (a) $D = 0$ (b) $D = 1$ (c) $D \approx D_c$ (d) $D = 5$ ($D_c \simeq 3.88458$). All parameters are dimensionless.

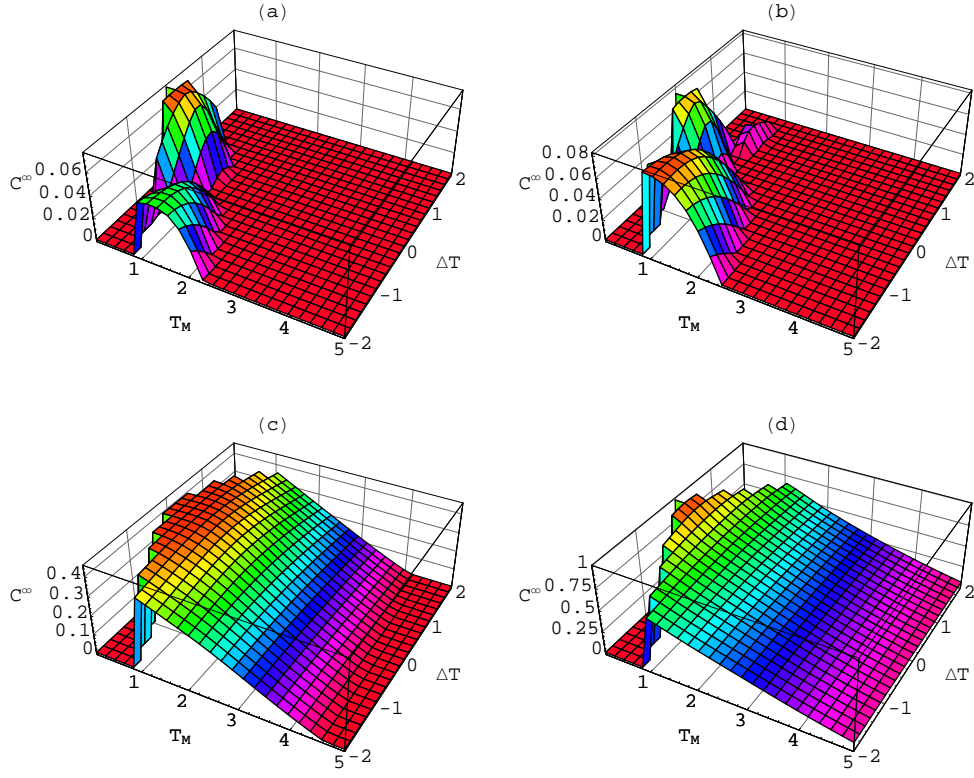


FIG. 7: (Color online) Asymptotic entanglement vs. T_M and ΔT . The parameters of the model are chosen to be $\gamma_1 = \gamma_2 = 0.02$, $B = 4$, $J = 1$, $\chi = 0.3$ and $b = 1$ for (a) $D = 0$ (b) $D = 1$ (c) $D \approx D_c$ (d) $D = 5$ ($D_c \simeq 3.75366$). All parameters are dimensionless.